

Squeezing and Entanglement of Density Oscillations in a Bose-Einstein Condensate

Andrew C. J. Wade, Jacob F. Sherson, and Klaus Mølmer

Department of Physics and Astronomy, Aarhus University, Ny Munkegade 120, DK-8000 Aarhus C, Denmark

(Received 16 April 2015; published 3 August 2015)

The dispersive interaction of atoms and a far-detuned light field allows nondestructive imaging of the density oscillations in Bose-Einstein condensates. Starting from a ground state condensate, we investigate how the measurement backaction leads to squeezing and entanglement of the quantized density oscillations. We show that properly timed, stroboscopic imaging and feedback can be used to selectively address specific eigenmodes and avoid excitation of nontargeted modes of the system.

DOI: 10.1103/PhysRevLett.115.060401

PACS numbers: 03.75.Gg

Squeezed and entangled states of light are important ingredients in quantum metrology and communication [1,2]. Production of analogous states of matter has been a long quest in physics with implementations demonstrated in atomic ensembles, as well as in superconducting and nanomechanical devices. Relying on nonlinearities due to atomic interactions, ultracold atoms have been prepared in entangled states of split atomic clouds [3,4] and internal state components [5–10], and in states that violate classical inequalities [11–16].

Using dispersive light-matter interactions and measurement backaction, room temperature vapor experiments have demonstrated squeezed [17] and entangled [18] states, quantum teleportation [19], and a quantum memory for light [20]. Similar experiments with interacting cold atoms and light fields have shown great progress [21–24], and numerous proposals exist [25–27] to manipulate the collective quantum states of ultracold atoms, while full exploitation of the quantum nature of the interaction and measurements is yet to be realized.

In this Letter we develop a theoretical treatment of Bose-Einstein condensate (BEC) dynamics due to the dispersive interaction with an optical probe field and feedback [Fig. 1(a)]. We investigate the selective preparation of squeezed and entangled states of the multimodal excitations of the BEC. The local atomic density is not a quantum nondemolition (QND) variable, but by applying stroboscopic measurements at selected times, we can address effective QND variables of selected eigenmodes of the BEC dynamics [28–30].

Atomic system.—We consider a 1D ultracold Bose gas [31] harmonically confined with axial (radial) trapping frequency $\omega_{x(\perp)}$ and length scale $l_{x(\perp)} = \sqrt{\hbar/m\omega_{x(\perp)}}$ [Fig. 1(a)], where radially tight confinement restricts the low-energy excitations to axial motion. The BEC ground state wave function $f_0(x)$ (taken to be real) is given by the 1D Gross-Pitaevskii equation

$$[H_{1D} + g_{1D}n_0(x)]f_0(x) = \mu f_0(x),$$

where the BEC meanfield density is $n_0(x) = Nf_0^2(x)$, and the chemical potential μ enforces the BEC population to the total number of atoms N . H_{1D} is the single atom Hamiltonian with the potential $V(x) = m\omega_x^2 x^2/2$. The interaction strength is $g_{1D} = 2\hbar^2 a_{sc}/m l_{\perp}^2$ with the s -wave scattering length a_{sc} . The elementary excitations of the BEC are the collective center-of-mass, breathing, and higher order modes, where each mode j constitutes a quantum harmonic oscillator degree of freedom with the dimensionless quadrature observables $\hat{x}_j(t)$ and $\hat{p}_j(t)$ with $[\hat{x}_j(t), \hat{p}_k(t)] = i\delta_{jk}$. Their frequencies ω_j and wave functions $f_j^{\pm}(x)$ are found by solution of the Bogoliubov–de Gennes equations

$$\begin{bmatrix} 0 & \mathcal{L}_+ \\ \mathcal{L}_- & 0 \end{bmatrix} \begin{bmatrix} f_j^+(x) \\ f_j^-(x) \end{bmatrix} = \hbar\omega_j \begin{bmatrix} f_j^+(x) \\ f_j^-(x) \end{bmatrix},$$

where $\mathcal{L}_{\pm} = H_{1D} - \mu + (2 \pm 1)g_{1D}n_0(x)$. These eigenmodes provide an expansion of the probed atomic density

$$\hat{n}(x, t) = n_0(x) + 2 \sum_j \sqrt{n_0(x)} f_j^-(x) \hat{x}_j(t) + O(N^0), \quad (1)$$

embodying the dynamic quantum fluctuations about the BEC meanfield. As we shall see, stroboscopically probing the density enables mode selective squeezing [red line in Fig. 1(b)] and entanglement [nonzero off-diagonal elements in Fig. 1(c,ii)], and reinitialization of the modes to oscillator ground states [end of the sequence in Fig. 1(b)].

Measurement.—The dispersive light-matter interaction is characterized by the coupling constant $\kappa = -\sqrt{d_0}\eta$ with the atomic depumping rate η and optical depth d_0 [32]. As we image the spatial density (1) by optical phase shift measurements [Fig. 1(a)], the light field detection in a pixel is sensitive to (a combination of) the atomic variables $\hat{x}_j(t)$ described by the atomic-pixel mode overlap integrals

$$\bar{f}_{jd} = \int_d dx \int dx' \mathcal{K}_1(x - x') f_0(x') f_j^-(x'),$$

where $\int_d dx$ denotes integration over the domain of the d th pixel. The convolution with the measurement kernel,

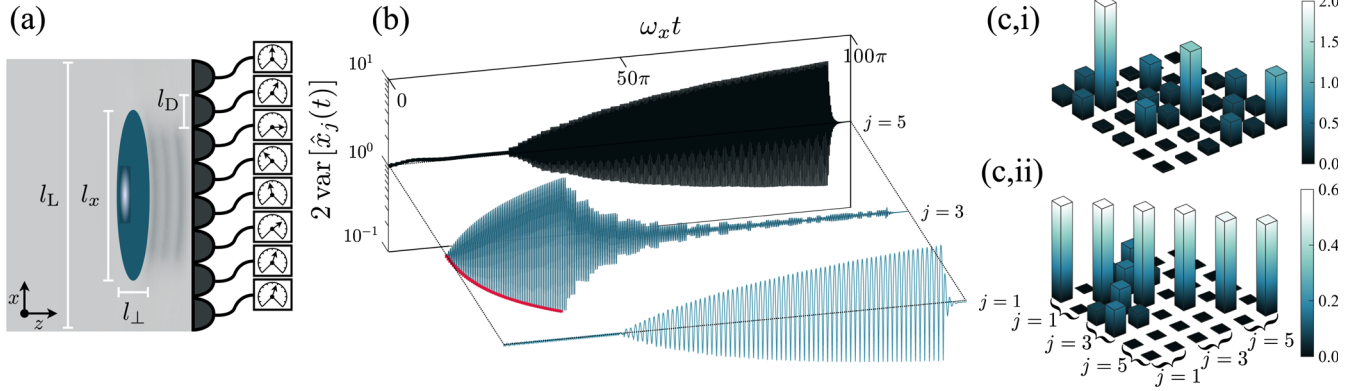


FIG. 1 (color online). (a) A BEC imprints a phase shift on a planar coherent light field depending on the atomic density along the BEC axis. The phase shifts are spatially detected by an encapsulating ($l_L > l_x$) array of homodyne detectors (pixels) of widths $l_D = l_x/10$. (b) The atomic modes can be selectively addressed and squeezed, illustrated here, where first the 3rd mode, and subsequently, modes 1 and 5 are squeezed. (c) The absolute value of the covariance matrix elements for the first three odd modes. Continuous probing (i) squeezes and correlates a swathe of atomic modes, while stroboscopic probing (ii) can generate correlations between only selected modes. The same level of entanglement of modes 1 and 3 is achieved in (i) and (ii), while the strong squeezing and the addressing of the 5th mode in (i) is absent in (ii). See text for the pulse sequences. The simulations are for the D_2 line (σ_+ polarized) of 1000 ^{87}Rb atoms in the $|F, F_z\rangle = |2, 2\rangle$ state with $\omega_x = 2\pi \times 150$ Hz, $\omega_\perp = 100\omega_x$, and $\mu = 2\hbar\omega_x$.

$\mathcal{K}_\alpha(x) = \int dk e^{-[(\alpha k)^4/64\pi^2]} e^{ikx}/2\pi$ [33,34], accounts for the resolution limit along the BEC axis associated with diffraction of light propagating over distances $\sim l_\perp$ through the BEC. By smearing out spatial features smaller than $l_R = (l_\perp \lambda)^{1/2}$, where λ is the light wavelength, it prevents the addressing of modes with shorter spatial variations that scale as $\sim l_x/j$. For our analysis of correlations between atomic modes, we will also need the overlap integrals

$$\bar{f}_{jk}^2 = \int dx \int dx' \mathcal{K}_{\sqrt{2}}(x-x') f_0(x) f_j^-(x) f_0(x') f_k^-(x').$$

Since the dominant contributions of the light-matter interaction are second order in light and atomic quadratures and the light field is subject to quadrature measurements, the quantum state can be described by a Gaussian state [35]. The state is fully characterised by the first, $[\mathbf{R}]_j = \langle \hat{\mathbf{v}}_j \rangle$, and second, $[\mathbf{A}]_{jk} = \text{cov}(\hat{\mathbf{v}}_j, \hat{\mathbf{v}}_k)$, moments of the atomic mode variables, $\hat{\mathbf{v}} = [\hat{x}_1(t), \hat{p}_1(t), \hat{x}_2(t), \hat{p}_2(t), \dots]^T$. Following the methodologies of [36], the quantum backaction of the light field measurements of the \hat{p} quadrature in each pixel [represented by expectation values and random Wiener increments, $dW_a(t)$] results in the stochastic evolution of the displacements (first moments) [37]

$$d\mathbf{R} = -\mathbf{D}\mathbf{R}dt + \mathbf{A}d\mathbf{W}. \quad (2)$$

The harmonic rotation in all $\{\hat{x}_j(t), \hat{p}_j(t)\}$ phase spaces is represented by the block diagonal matrix \mathbf{D} of blocks

$$[\mathbf{D}]_j = \begin{bmatrix} 0 & -\omega_j \\ \omega_j & 0 \end{bmatrix}.$$

Each pixel probes a linear combination of modes represented by a rectangular matrix of blocks

$$[\mathbf{M}]_{jd} = -\sqrt{\frac{l_L}{l_D}} \begin{bmatrix} 0 & 2\kappa \bar{f}_{jd} \\ 0 & 0 \end{bmatrix},$$

and owing to the correlations among the modes (A), the measurement results $d\mathbf{W} = [0, dW_1(t), 0, dW_2(t), \dots]^T$ affect the modes in a correlated manner.

The covariance matrix (second moments) evolve as [37]

$$\dot{\mathbf{A}} = \mathbf{E} - \mathbf{D}\mathbf{A} - \mathbf{A}\mathbf{D}^T - \mathbf{A}\mathbf{M}\mathbf{M}^T\mathbf{A}, \quad (3)$$

where the square matrix of blocks

$$[\mathbf{E}]_{jk} = \begin{bmatrix} 0 & 0 \\ 0 & \kappa^2 l_L \bar{f}_{jk}^2 \end{bmatrix}.$$

\mathbf{A} evolves independently of the measurement outcomes. While this implies that we can deterministically assess the squeezing and entanglement in the system, the random measurement results determine the displacements, about which the squeezing and entanglement occurs. We first consider the solution of Eq. (3), focusing on the squeezing and entanglement generation, and later return to the stochastic evolution of the displacements described by Eq. (2).

Squeezing.—Continuous probing with strength κ squeezes $\hat{x}_j(t)$ at a rate $\nu_j = \kappa^2 l_L \bar{f}_{jj}^2$, while the conjugate quadrature $\hat{p}_j(t)$ is antisqueezed. Since $\hat{x}_j(t)$ and $\hat{p}_j(t)$ are coupled by rotation at a rate ω_j , the squeezing is restricted. Thus, the maximal squeezing of $\hat{x}_j(t)$ occurs within the first quarter of a full phase-space rotation. In the long-time limit, Eq. (3) yields a steady-state solution where the $\hat{x}_j(t)$ variance, $\text{var}[\hat{x}_j(t)]_{\text{SS}} \approx [(1 + 4\bar{\nu}_j^2)^{1/2} - 1]^{1/2}/2\sqrt{2}\bar{\nu}_j \leq 1/2$, is determined by the rotation and squeezing rates, $\bar{\nu}_j = \nu_j/\omega_j$. Alternatively squeezing the \hat{x}_j^0 quadrature of the time dependent $\hat{x}_j(t) = \hat{x}_j^0 \cos \omega_j t + \hat{p}_j^0 \sin \omega_j t$ is possible by

applying a temporally modulated field [38] with a sequence of constant intensity pulses determined by one or more frequencies ϖ_i . The timings t_l and durations τ_l of the pulses are determined by ensuring, for each frequency, that $\varpi_i t$ is within $\Delta\phi/2$ from a multiple of 2π . Probing at the single frequency $\varpi = 2\omega_j$ amounts to a train of n pulses centered on times $t_l = [0, \pi/\omega_j, 2\pi/\omega_j, \dots, n\pi/\omega_j]$ with identical durations, $\tau_l = \tau = \Delta\phi/\varpi$. Such a field squeezes the $\pm\hat{x}_j^0$ quadrature, while avoiding its antisqueezing at intermediate times. This enables squeezing well beyond the continuous case for the same strength κ . For small $\Delta\phi$, effective QND probing of \hat{x}_j^0 is expected, $\text{var}[\hat{x}_j^0]_{\text{QND}} = 1/2(1 + 2\nu_j\tau_T)$ [39] with $\tau_T = n\tau$, and is observed (red line) in Fig. 1(b) where the first quarter of the trace squeezes the 3rd mode ($\kappa^2 = 100\omega_x/2\pi$, $\varpi = 2\omega_3$, and $\Delta\phi/2\pi = 0.05$).

The atomic multimodal system is far from the single-mode squeezing picture. However, if no other mode nor coupled correlation has a rational frequency ratio to ω_j , the pulse train only addresses the j th mode. This modal selectivity is illustrated in Fig. 1(b), where the variances of modes 1 and 5 are essentially unaffected during probing of the 3rd mode. Here, the atomic interactions provide an irregular spectrum of mode frequencies [31], allowing separate addressing without crosstalk.

The simultaneous squeezing of two modes, j and k , is achieved with the two frequencies, $\varpi_1 = 2\omega_j$ and $\varpi_2 = 2\omega_k$, as featured in Fig. 1(b) for modes 1 and 5 after the time $\omega_x t = 25\pi$ ($\Delta\phi/2\pi = 0.1$). The probing sequence is now out of phase with the 3rd mode, and hence, its prior squeezing is progressively lost, returning to initial vacuum values. The final 5% of the sequence demonstrates reinitialization of all modes to vacuum fluctuations by switching to weak continuous probing ($\kappa^2 = 50\omega_x/2\pi$). The preservation of vacuum fluctuations of the nontargeted modes, the loss of squeezing of the 3rd mode, and the reinitialization of all modes to vacuum fluctuations, featured in Fig. 1(b), are demonstrations of the interplay between atomic dynamics, measurement strength, and stroboscopic probing, enacting a quantum eraser.

To further assess the performance of the operations, we study squeezing of the 3rd mode in Fig. 2 (similar results are found for other modes and for the joint squeezing or entangling of pairs of modes). The rate of squeezing is determined by $\Delta\phi$, as the accumulated probing time $\tau_T \propto \Delta\phi$ (inset). However, only for smaller $\Delta\phi$, the x quadrature is probed in a QND fashion (red line), while the squeezing for larger $\Delta\phi$ is suboptimal as a result of the inadvertent probing of the p component. The figure also addresses crosstalk between the $j = 1, 3, 5$ subsystem and its complement through the purity P of its reduced density matrix $\hat{\rho}$. The Hellinger distance $D_{\mathcal{H}} = \text{Tr}[\hat{\rho}^{1/2} - (\hat{\rho}_d)^{1/2}]^2/2$ [40] quantifies the selectivity within the subsystem. The desired state $\hat{\rho}_d$ assumes identical \mathbf{R} to $\hat{\rho}$, but with all blocks $[\mathbf{A}]_{jk}$, except $j = k = 3$, replaced by their initial vacuum values. Excellent selectivity ($D_{\mathcal{H}} \approx 0$) and little crosstalk ($P \approx 1$)

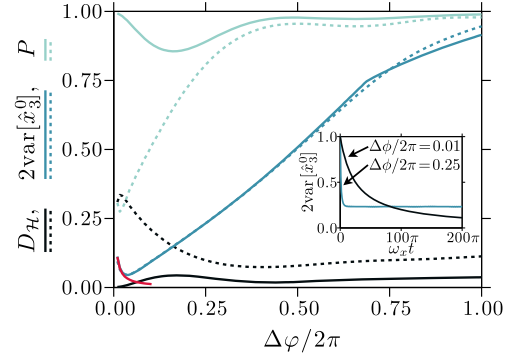


FIG. 2 (color online). The squeezing of the 3rd mode after stroboscopically probing ($\kappa^2 = 100\omega_x/2\pi$) for 100 trap periods is shown, while the temporal evolution of the quadrature variance $\text{var}[\hat{x}_3^0]$ is illustrated in the inset. Dotted lines indicate the results of the noninteracting atomic system for comparison. For small $\Delta\phi$ (pulse duration), $\text{var}[\hat{x}_3^0]$ follows the QND result (red line, see text), while for larger $\Delta\phi$, the squeezing is faster but suboptimal. Excellent selectivity, Hellinger distance $D_{\mathcal{H}} \approx 0$, and little crosstalk, Purity $P \approx 1$, are observed for small $\Delta\phi$.

are observed for small $\Delta\phi$. For comparison (dotted lines), a noninteracting atomic system demonstrates similar squeezing; however, the corresponding linear spectrum $\omega_j = \omega_x j$ results in significant crosstalk and poor mode selectivity.

Entanglement.—A probe transmitted through two atomic media reveals information about their collective rather than individual properties and may hence lead to their mutual entanglement [39]. Similarly, we may entangle two modes, j and k , of a single BEC by probing the density in a manner that does not discriminate contributions from the individual modes. The modes' respective spatial signatures, $\sim f_0(x)f_j^-(x)$ and $\sim f_0(x)f_k^-(x)$, must be indistinct ($\tilde{f}_{jk}^2 \neq 0$). Partial temporal distinguishability, owing to different oscillation frequencies ω_j and ω_k , is avoided by stroboscopically probing with a train of pulses at the single frequency $\varpi = \omega_j + \omega_k$. Analogous to the case of squeezing, it also allows selective addressing of modes as illustrated in Fig. 1(c). The absolute value of the covariance matrix elements of the $j = 1, 3, 5$ subsystem is shown for (i) the steady state of continuous probing ($\kappa^2 = 1000\omega_x/2\pi$) and (ii) stroboscopic probing for 100 trap periods ($\kappa^2 = 4\omega_x/2\pi$ and $\Delta\phi/2\pi = 0.03$). Although both cases reach the same level of entanglement of modes 1 and 3, the continuous probing requires a larger strength κ , addresses a swathe of modes, and causes significant squeezing.

Bipartite entanglement can be quantified by the logarithmic negativity $E_{jk} = \log_2 \|\hat{\rho}_B^{TP}\|_{\text{Tr}}$ [35] of the bipartite reduced density matrix $\hat{\rho}_B$, where TP denotes the partial transpose and $\|\cdot\|_{\text{Tr}}$ the trace norm. Figure 3(a) shows the entanglement between modes 1 and 3, and the comparison to an effective QND probing, for $\kappa^2\tau \rightarrow \infty$ $E_{\text{QND}}^{13} \rightarrow \log_4[(1 + \beta_{jk}/1 - \beta_{jk})]$. The spatial distinguishability of

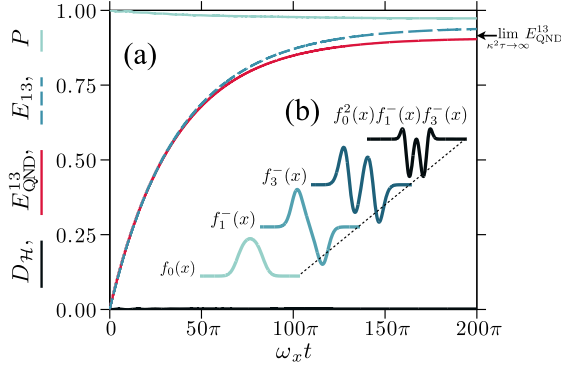


FIG. 3 (color online). (a) Modes 1 and 3 are entangled by a pulse sequence of 100 trap periods with $\varpi_1 = \omega_1 + \omega_3$, $\Delta\phi/2\pi = 0.03$, and $\kappa^2 = 30\omega_x/2\pi$. The logarithmic negativity E_{13} slightly outperforms the corresponding QND result E_{QND}^{13} . The selectivity within the $j = 1, 3, 5$ subsystem is excellent ($D_{\mathcal{H}} \approx 0$) and the subsystem's purity is $P \sim 97\%$. (b) The mode functions (not to scale) of the condensate $f_0(x)$, entangled modes $f_{1,3}^-(x)$, and the overlap $\sim f_0^2(x)f_1^-(x)f_3^-(x)$.

the mode functions, Fig. 3(b), remains the limiting factor and is parameterized by $\beta_{jk} = |\tilde{f}_{jk}^2|/|\tilde{f}_{jj}^2 \tilde{f}_{kk}^2|^{1/2}$. Deviations from E_{QND}^{13} and a small loss of purity, $P \sim 97\%$, are attributed to coupling to other modes with commensurate correlation frequencies [here, $\omega_1 + \omega_3 \approx (\omega_1 + \omega_7)/2$]. The selectivity within the subsystem is excellent, $D_{\mathcal{H}} \approx 0$, where $\hat{\rho}_d$ is identical to $\hat{\rho}$, except initial vacuum covariances of the 5th mode.

Feedback.—We have demonstrated that stroboscopic probing permits squeezing and entanglement of particular resonant modes. As illustrated in Fig. 4(a), the modes are also subject to random displacements due to the diffusion terms in Eq. (2). These coherent displacements of the mean field correspond to a modification of the Gross-Pitaevskii meanfield wave function. A micromirror array [41], a spatial light modulator [42], or an acousto-optic deflector [43] can provide adaptive lightshift potentials for the atoms and serve as a feedback mechanism to recover and maintain the original condensate wave function $f_0(x)$. Mode matching with the single atom Hamiltonian $H_f = \hbar \sum_k h_k(x) \langle \hat{p}_k(t) \rangle$, where $h_k(x) = 2\omega_j f_j^+(x) \delta_{jk} / \sqrt{n_0(x)}$, we can selectively address the displacement of the j th mode and

$$[\mathbf{D}]_j \rightarrow \begin{bmatrix} 0 & -\omega_j \\ \omega_j & 2\omega_j \end{bmatrix}$$

is changed in Eq. (2). The deterministic evolution of $\hat{x}_j(t)$ and $\hat{p}_j(t)$ becomes critically damped, suppressing the displacements caused by the $d\mathbf{W}$ terms in Eq. (2). Simulating the full multimode dynamics, Fig. 4(b) demonstrates that the displacement of the squeezed mode in Fig. 2 is successfully suppressed.

The feedback demonstrated in Fig. 4 is only performed for a single mode. In the effective QND examples of

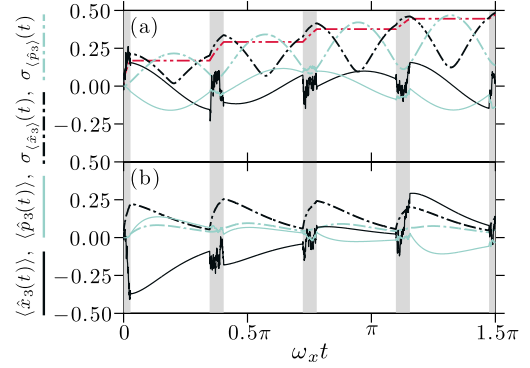


FIG. 4 (color online). A stochastic trajectory of $\langle \hat{x}_3(t) \rangle$ and $\langle \hat{p}_3(t) \rangle$, and the standard deviations of 1000 trajectories $\sigma_{\langle \hat{x}_3 \rangle}(t)$ and $\sigma_{\langle \hat{p}_3 \rangle}(t)$, corresponding to Fig. 2 ($\Delta\phi/2\pi = 0.15$). The gray regions indicate when the measurement occurs. (a) Without feedback, the trajectories diffuse and oscillate, and approximately $\sigma_{\langle \hat{x}_3 \rangle}(t) = \sigma_{\langle \hat{p}_3 \rangle}(t) = \sqrt{\nu_3 \tau_T / 2}$ (red line). (b) With feedback, the desired damping of displacements is demonstrated.

single-mode squeezing (e.g., $\Delta\phi = 0.01$ in Fig. 2) and bipartite entanglement (Fig. 3), the coherent displacement of the modes corresponds to an $\sim 8\%$ population N_{nc} outside of the BEC mode. If necessary, more elaborate H_f can be investigated to simultaneously minimize the excitation of multiple modes, and N_{nc} may be reduced by different trapping geometries, where the measurement kernel $\mathcal{K}_\alpha(x)$ may yield less coherent excitation of the irrelevant modes.

Conclusions.—We have demonstrated the quantum control of a matter-wave system via spatially resolved optical probing and feedback. Using stroboscopic probing, we can address and correlate effective QND observables of selected density modes of a BEC, while preserving the initial vacuum fluctuations of nontargeted modes. Our method of spatially resolved imaging may hold similar prospects for squeezing and entanglement in other quantum many-body systems with harmonic excitation modes, such as, e.g., the center-of-mass Kohn mode [44], breathing modes of the Tonks-Girardeau gas [45], full quantum 2D systems [46], and the unitary 3D quantum gas [47]. In any of these cases the performance relies on independent excitation modes, and it is ultimately limited by the residual atomic depumping [32]. For small 1D alkali condensates we estimate that experimental parameters, currently available [48–50], permit significant squeezing and entanglement of the selected modes.

A. C. J. W. and K. M. acknowledge support from the Villum Foundation Center of Excellence, QUSCOPE, and the E. U. Marie Curie program ITN-Coherence 265031. J. F. S. acknowledges support from Lundbeckfonden and the Danish Council for Independent Research. A. C. J. W. wishes to thank C. K. Andersen and M. C. Tichy for fruitful discussions, and R. Blattmann, A. H. Kiilerich, and Q. Xu for feedback on the manuscript.

- [1] L.-A. Wu, H. J. Kimble, J. L. Hall, and H. Wu, Generation of Squeezed States by Parametric Down Conversion, *Phys. Rev. Lett.* **57**, 2520 (1986).
- [2] A. Furusawa, J. L. Sørensen, S. L. Braunstein, C. A. Fuchs, H. J. Kimble, and E. S. Polzik, Unconditional quantum teleportation, *Science* **282**, 706 (1998).
- [3] J. Estève, C. Gross, A. Weller, S. Giovanazzi, and M. Oberthaler, Squeezing and entanglement in a Bose-Einstein condensate, *Nature (London)* **455**, 1216 (2008).
- [4] T. Berrada, S. van Frank, R. Bücker, T. Schumm, J.-F. Schaff, and J. Schmiedmayer, Integrated Mach-Zehnder interferometer for Bose-Einstein condensates, *Nat. Commun.* **4**, 2077 (2013).
- [5] M. Riedel, P. Böhi, Y. Li, T. Hänsch, A. Sinatra, and P. Treutlein, Atom-chip-based generation of entanglement for quantum metrology, *Nature (London)* **464**, 1170 (2010).
- [6] C. Gross, H. Strobel, E. Nicklas, T. Zibold, N. Bar-Gill, G. Kurizki, and M. Oberthaler, Atomic homodyne detection of continuous-variable entangled twin-atom states, *Nature (London)* **480**, 219 (2011).
- [7] C. Hamley, C. Gerving, T. Hoang, E. Bookjans, and M. Chapman, Spin-nematic squeezed vacuum in a quantum gas, *Nat. Phys.* **8**, 305 (2012).
- [8] B. Lücke, M. Scherer, J. Kruse, L. Pezz, F. Deuretzbacher, P. Hyllus, O. Topic, J. Peise, W. Ertmer, J. Arlt, L. Santos, A. Smerzi, and C. Klempt, Twin matter waves for interferometry beyond the classical limit, *Science* **334**, 773 (2011).
- [9] C. Gross, T. Zibold, E. Nicklas, J. Estève, and M. Oberthaler, Nonlinear atom interferometer surpasses classical precision limit, *Nature (London)* **464**, 1165 (2010).
- [10] W. Muessel, H. Strobel, D. Linnemann, D. B. Hume, and M. K. Oberthaler, Scalable Spin Squeezing for Quantum-Enhanced Magnetometry with Bose-Einstein Condensates, *Phys. Rev. Lett.* **113**, 103004 (2014).
- [11] J. M. Vogels, K. Xu, and W. Ketterle, Generation of Macroscopic Pair-Correlated Atomic Beams by Four-Wave Mixing in Bose-Einstein Condensates, *Phys. Rev. Lett.* **89**, 020401 (2002).
- [12] A. Perrin, H. Chang, V. Krachmalnicoff, M. Schellekens, D. Boiron, A. Aspect, and C. I. Westbrook, Observation of Atom Pairs in Spontaneous Four-Wave Mixing of Two Colliding Bose-Einstein Condensates, *Phys. Rev. Lett.* **99**, 150405 (2007).
- [13] M. Keller, M. Kotyrba, F. Leupold, M. Singh, M. Ebner, and A. Zeilinger, Bose-Einstein condensate of metastable helium for quantum correlation experiments, *Phys. Rev. A* **90**, 063607 (2014).
- [14] K. V. Kheruntsyan, J.-C. Jaskula, P. Deuar, M. Bonneau, G. B. Partridge, J. Ruaudel, R. Lopes, D. Boiron, and C. I. Westbrook, Violation of the Cauchy-Schwarz Inequality with Matter Waves, *Phys. Rev. Lett.* **108**, 260401 (2012).
- [15] R. J. Lewis-Swan and K. V. Kheruntsyan, Proposal for demonstrating the Hong-Ou-Mandel effect with matter waves, *Nat. Commun.* **5**, 3752 (2014).
- [16] R. Lopes, A. Imanaliev, A. Aspect, M. Cheneau, D. Boiron, and C. I. Westbrook, Atomic Hong-Ou-Mandel experiment, *Nature (London)* **520**, 66 (2015).
- [17] A. Kuzmich, L. Mandel, and N. P. Bigelow, Generation of Spin Squeezing via Continuous Quantum Nondemolition Measurement, *Phys. Rev. Lett.* **85**, 1594 (2000).
- [18] B. Julsgaard, A. Kozhekin, and E. S. Polzik, Experimental long-lived entanglement of two macroscopic objects, *Nature (London)* **413**, 400 (2001).
- [19] J. Sherson, H. Krauter, R. Olsson, B. Julsgaard, K. Hammerer, I. Cirac, and E. Polzik, Quantum teleportation between light and matter, *Nature (London)* **443**, 557 (2006).
- [20] B. Julsgaard, J. Sherson, J. I. Cirac, J. Fiurasek, and E. Polzik, Experimental demonstration of quantum memory for light, *Nature (London)* **432**, 482 (2004).
- [21] D. M. Stamper-Kurn, A. P. Chikkatur, A. Görlitz, S. Inouye, S. Gupta, D. E. Pritchard, and W. Ketterle, Excitation of Phonons in a Bose-Einstein Condensate by Light Scattering, *Phys. Rev. Lett.* **83**, 2876 (1999).
- [22] J. Denschlag, J. E. Simsarian, D. L. Feder, C. W. Clark, L. A. Collins, J. Cubizolles, L. Deng, E. W. Hagley, K. Helmerson, W. P. Reinhardt, S. L. Rolston, B. I. Schneider, and W. D. Phillips, Generating solitons by phase engineering of a Bose-Einstein condensate, *Science* **287**, 97 (2000).
- [23] M. Saba, T. A. Pasquini, C. Sanner, Y. Shin, W. Ketterle, and D. E. Pritchard, Light scattering to determine the relative phase of two Bose-Einstein condensates, *Science* **307**, 1945 (2005).
- [24] C. Sanner, E. J. Su, A. Keshet, W. Huang, J. Gillen, R. Gommers, and W. Ketterle, Speckle Imaging of Spin Fluctuations in a Strongly Interacting Fermi Gas, *Phys. Rev. Lett.* **106**, 010402 (2011).
- [25] I. B. Mekhov and H. Ritsch, Quantum optics with ultracold quantum gases: towards the full quantum regime of the light-matter interaction, *J. Phys. B* **45**, 102001 (2012).
- [26] M. Hush, S. Szigeti, A. Carvalho, and J. Hope, Controlling spontaneous-emission noise in measurement-based feedback cooling of a Bose-Einstein condensate, *New J. Phys.* **15**, 113060 (2013).
- [27] M. D. Lee and J. Ruostekoski, Classical stochastic measurement trajectories: Bosonic atomic gases in an optical cavity and quantum measurement backaction, *Phys. Rev. A* **90**, 023628 (2014).
- [28] V. B. Braginskii, Y. I. Vorontsov, and F. Y. Khalili, *Zh. Eksp. Teor. Fiz.* **27**, 291 (1978) [Optimal quantum measurements in detectors of gravitation radiation, *JETP Lett.* **27**, 276 (1978)].
- [29] K. S. Thorne, R. W. P. Drever, C. M. Caves, M. Zimmermann, and V. D. Sandberg, Quantum Nondemolition Measurements of Harmonic Oscillators, *Phys. Rev. Lett.* **40**, 667 (1978).
- [30] V. B. Braginskii, Y. I. Vorontsov, and K. S. Thorne, Quantum nondemolition measurements, *Science* **209**, 547 (1980).
- [31] D. Petrov, D. M. Gangardt, and G. V. Shlyapnikov, Low-dimensional trapped gases, in *J. Phys. IV* **116**, 5 (2004).
- [32] K. Hammerer, A. S. Sørensen, and E. S. Polzik, Quantum interface between light and atomic ensembles, *Rev. Mod. Phys.* **82**, 1041 (2010).
- [33] D. A. R. Dalvit, J. Dziarmaga, and R. Onofrio, Continuous quantum measurement of a Bose-Einstein condensate: A stochastic Gross-Pitaevskii equation, *Phys. Rev. A* **65**, 053604 (2002).
- [34] S. S. Szigeti, M. R. Hush, A. R. R. Carvalho, and J. J. Hope, Continuous measurement feedback control of a Bose-Einstein condensate using phase-contrast imaging, *Phys. Rev. A* **80**, 013614 (2009).

- [35] C. Weedbrook, S. Pirandola, R. García-Patrón, N. J. Cerf, T. C. Ralph, J. H. Shapiro, and S. Lloyd, Gaussian quantum information, *Rev. Mod. Phys.* **84**, 621 (2012).
- [36] L. B. Madsen and K. Mølmer, Spin squeezing and precision probing with light and samples of atoms in the Gaussian description, *Phys. Rev. A* **70**, 052324 (2004).
- [37] Details to be presented elsewhere.
- [38] G. Vasilakis, H. Shen, K. Jensen, M. Balabas, D. Salart, B. Chen, and E. S. Polzik, Generation of a squeezed state of an oscillator by stroboscopic back-action-evading measurement, *Nat. Phys.* **11**, 389 (2015).
- [39] L.-M. Duan, J. I. Cirac, P. Zoller, and E. S. Polzik, Quantum Communication between Atomic Ensembles Using Coherent Light, *Phys. Rev. Lett.* **85**, 5643 (2000).
- [40] P. Marian and T. A. Marian, Hellinger distance as a measure of Gaussian discord, *J. Phys. A* **48**, 115301 (2015).
- [41] S. A. Goorden, J. Bertolotti, and A. P. Mosk, Superpixel-based spatial amplitude and phase modulation using a digital micromirror device, *Opt. Express* **22**, 17999 (2014).
- [42] D. McGloin, G. Spalding, H. Melville, W. Sibbett, and K. Dholakia, Applications of spatial light modulators in atom optics, *Opt. Express* **11**, 158 (2003).
- [43] C. Ryu, P. W. Blackburn, A. A. Blinova, and M. G. Boshier, Experimental realization of Josephson Junctions for an atom SQUID, *Phys. Rev. Lett.* **111**, 205301 (2013).
- [44] J. Reidl, G. Bene, R. Graham, and P. Szépfalussy, Kohn mode for trapped Bose gases within the dielectric formalism, *Phys. Rev. A* **63**, 043605 (2001).
- [45] C. Menotti and S. Stringari, Collective oscillations of a one-dimensional trapped Bose-Einstein gas, *Phys. Rev. A* **66**, 043610 (2002).
- [46] L. P. Pitaevskii and A. Rosch, Breathing modes and hidden symmetry of trapped atoms in two dimensions, *Phys. Rev. A* **55**, R853 (1997).
- [47] F. Werner and Y. Castin, Unitary gas in an isotropic harmonic trap: Symmetry properties and applications, *Phys. Rev. A* **74**, 053604 (2006).
- [48] A. Widera, S. Trotzky, P. Cheinet, S. Fölling, F. Gerbier, I. Bloch, V. Gritsev, M. D. Lukin, and E. Demler, Quantum Spin Dynamics of Mode-Squeezed Luttinger Liquids in Two-Component Atomic Gases, *Phys. Rev. Lett.* **100**, 140401 (2008).
- [49] T. Langen, R. Geiger, M. Kuhnert, B. Rauer, and J. Schmiedmayer, Local emergence of thermal correlations in an isolated quantum many-body system, *Nat. Phys.* **9**, 640 (2013).
- [50] E. Haller, M. Gustavsson, M. J. Mark, J. G. Danzl, R. Hart, G. Pupillo, and H.-C. Nägerl, Realization of an excited, strongly correlated quantum gas phase, *Science* **325**, 1224 (2009).